AIMS Mathematics, 9(1): 1088–1102.
DOI: 10.3934/math.2024053
Received: 04 October 2023
Revised: 18 November 2023
Accepted: 27 November 2023
Published: 06 December 2023

http://www.aimspress.com/journal/Math

Research article

Time-delayed feedback control for chaotic systems with coexisting attractors

Erxi Zhu[1,2,*]

[1] College of Internet of Things Engineering, Jiangsu Vocational College of Information Technology, Wuxi 214153, China

[2] College of Computer Science and Technology, Nanjing University of Aeronautics and Astronautics, Nanjing 211106, China

* **Correspondence:** Email: erxi666@163.com.

Abstract: This study investigated the Hopf bifurcation of the equilibrium point of chaotic systems with coexisting attractors under the time-delayed feedback control. First, the equilibrium point and Hopf bifurcation of chaotic systems with coexisting attractors were analyzed. Second, the chaotic systems were controlled by time-delayed feedback, the transversality condition of Hopf bifurcation at the equilibrium point was discussed, and the time-delayed value of Hopf bifurcation at the equilibrium point was obtained. Lastly, the correctness of the theoretical analysis was verified by using the numerical results.

Keywords: coexisting attractors; time-delayed feedback control; Hopf bifurcation; transverse condition
Mathematics Subject Classification: 93B52

1. Introduction

In engineering systems, the assessment of chaos [1] has been leaping forward over the past two decades. Chaos has shifted from merely a harmful phenomenon to a phenomenon considered to be of significance to practical applications. In addition, chaos has been extensively used in biomedical engineering, dynamic engineering [2] and chemical reaction engineering, which has aroused the attention from many scholars and encouraged their unremitting efforts for the research. Numerous researches indicated that the premise of chaos application is chaos control [3]. On the whole, an infinite number of unstable periodic orbits in the chaotic attractor have been commonly employed as the preferred target to convert the chaotic trajectory of the system to the anticipated periodic orbit or to stop the trajectory. Feedback control is the most concerned among considerable chaos control methods. It shows the advantages that it are not required to exploit any information regarding the given

controlled system (except for the output or state of the chaotic system), it does not alter the structure of the controlled system and it exhibits prominent track tracking ability and stability. However, its defects include that it requires a mathematical model and an input objective function or orbit with higher accuracy. There have been several notable chaotic feedback control methods (e.g., the parameter perturbation method [4], the continuous feedback control method [5] [the external force feedback control method and the time-delayed feedback control method], the adaptive control method [6], as well as the sliding mode variable structure control method [7]).

The time-delayed feedback control method refers to a vital chaos control method. It is not required to know the exact system model, which is incomparable to the parameter perturbation method. Besides, time-delayed phenomenon is universal in communication, ecology and many other systems. Over the past two years, views on the time-delayed feedback control of different dynamical systems have been extensively proposed. For instance, a novel robust time-delayed co-adaptive cruise control method was proposed for the vehicle queuing system with dynamic uncertainty and communication time-delayed variation [8]. In [9], an event-triggered static output feedback controller was proposed for the stabilization of linear systems with time-varying delays. In [10], two time-delayed feedback control methods were developed to stabilize the particle supply device that underwent the friction-induced vibration in the transmission belt. In [11], the time-delayed velocity feedback was introduced into the micro-nano electromechanical system. Li et al., [12] studied the distributed adaptive inclusion control problem of uncertain nonlinear multi-agent systems with time delays and unmodeled dynamics under fixed directed graphs. The mentioned literatures considered the time-delayed feedback control of low-dimensional chaotic systems, whereas they rarely studied the time-delayed feedback control of high-dimensional hyperchaotic systems. However, as compared with chaotic systems, hyperchaotic systems exhibit more complex dynamic behaviors, so they are of huge application significance in the field of secure communication. Given on the mentioned considerations, this study continued to study a category of 4D hyperchaotic systems with multiple coexisting attractors, presented a 4D hyperchaotic system model of the time-delayed feedback control and analyzed the stability of the equilibrium point as well as the parameter space and the delay value of Hopf bifurcation based on the unstable equilibrium point. This study is of certain theoretical value.

The rest of the study is organized as follows. In Section 1, the current research status quo of the time-delayed feedback control is analyzed. In Section 2, a 4D chaotic system model with coexisting attractors and its Hopf bifurcation analysis are presented. In Section 3, the 4D chaotic system of the time-delayed feedback control is introduced and the Hopf bifurcation analysis is conducted. In Section 4, the numerical simulation is performed to verify the correctness of the theoretical analysis. In Section 5, the work of this study is summarized.

2. Description of chaotic systems with coexisting attractors

In this section, we will analyze the origin of chaotic systems with arbitrary coexisting attractors and the stability of the system at the equilibrium point.

Among a wide range of chaotic systems [13, 14], there are multiple stable states covering multiple coexisting equilibrium states of multiple parameter sets, which refers to a chaotic system with coexisting attractors. In other words, under fixed parameters, its final state satisfies non-uniqueness as impacted by different initial conditions. Such a type of systems exhibits high flexibility and robustness,

and they are capable of realizing the transition between different states under appropriate control to adapt to various work scenarios [15–17]. In [18], a 4D hyperchaotic system with any number of coexisting chaotic attractors was built, which exhibited significantly complex dynamic behaviors. It was optimized from a simple memristor chaotic circuit with a nonlinear feedback control input u. The mathematical model of the memristor chaotic circuit [19] is expressed as:

$$\begin{cases} \dot{x} = y, \\ \dot{y} = -ax + by(1 - z^2), \\ \dot{z} = -y - cz + yz, \end{cases} \tag{2.1}$$

where a, b, c denote system parameters and x, y, z represent system variables. A 4D hyperchaotic system (2.1) was developed by implementing a nonlinear feedback control for $\sin(y)$ based on the system. The novel system (2.2) is written as:

$$\begin{cases} \dot{x} = y + u, \\ \dot{y} = -ax + by(1 - z^2), \\ \dot{z} = -y - cz + yz, \\ \dot{u} = \sin(y). \end{cases} \tag{2.2}$$

The Hopf bifurcation analysis for the system (2.3) is conducted below. First, the equilibrium point of the system is solved, and then the stability of the equilibrium point was discussed. Let

$$\begin{cases} y + u = 0, \\ -ax + by(1 - z^2) = 0, \\ -y - cz + yz = 0, \\ \sin(y) = 0. \end{cases} \tag{2.3}$$

The equilibrium point of the system is yielded: $S(x^*, y^*, z^*, u^*)$,

$$S = \begin{cases} x^* = \frac{bc^2y^* - 2bcy^{*2}}{a(y^* - c)^2}, \\ y^* = j\pi, \\ z^* = \frac{y^*}{y^* - c}, \\ u^* = -y^*, \end{cases} \qquad j = 0, \pm 1, \pm 2, \cdots. \tag{2.4}$$

Given the mentioned Eq (2.4), system (2.2) has an infinite number of equilibrium points, thereby demonstrating that the system (2.2) has any number of coexisting attractors. The characteristic equation of the system at the equilibrium point is expressed as:

$$\begin{vmatrix} -\lambda & 1 & 0 & 1 \\ -a & b(1 - z^{*2}) - \lambda & -2by^*z^* & 0 \\ 0 & z^* - 1 & y^* - c - \lambda & 0 \\ 0 & \cos(y^*) & 0 & -\lambda \end{vmatrix} = 0. \tag{2.5}$$

Equation (2.5) is transformed into

$$\lambda^4 + p_1\lambda^3 + p_2\lambda^2 + p_3\lambda + p_4 = 0, \tag{2.6}$$

where

$$p_1 = c - b(c+1)(1-z^{*2}),$$

$$p_2 = b(y^* - c)(1-z^{*2}),$$

$$p_3 = a + a\cos(y^*) + 2by^*z^{*2},$$

$$p_4 = a(\cos(y^*)+1)(c-y^*) - 2by^*z^*.$$

According to The Routh-Hurwitz criterion, to stabilize the system (2.2) at the equilibrium point $S(x^*, y^*, z^*, u^*)$, it should meet:

$$\begin{cases} p_1 > 0, \\ p_2 > 0, \\ p_3 > 0, \\ p_4 > 0, \\ p_1p_2 > p_3, \\ p_1p_2p_3 > p_3^2 + p_1^2p_4. \end{cases} \tag{2.7}$$

Overall, all the equilibrium points $S(x^*, y^*, z^*, u^*)$ should satisfy Eq (2.7), and the system parameter range can be obtained:

$$a > 0, b > 0, 0 < c < \pi.$$

Lemma 1. *When $a > 0$, $b > 0$, $0 < c < \pi$, the system* (2.2) *is stable at the equilibrium point $S(x^*, y^*, z^*, u^*)$, $j = \pm 1, \pm 2, \cdots$.*

In is noteworthy that at the equilibrium point $S(0, 0, 0, 0)$, the Eq (2.6) can be rewritten as:

$$\lambda^4 + (c - b - bc)\lambda^3 - bc\lambda^2 + 2a\lambda + 2ac = (\lambda + c)(\lambda^3 - b\lambda^2 + a\lambda + a) = 0. \tag{2.8}$$

Lemma 2. *When $a > 0$, $b > 0$, $0 < c < \pi$, the system is unstable at the equilibrium point $S(x^*, y^*, z^*, u^*)$. It is unstable when $j = 0$, and it undergoes Hopf bifurcation.*

When the parameters $a = 1$, $b = 1$, $c = 1$ and the initial conditions are $(1, 1, 1, 1)$, the roots of the characteristic equations of system (2.2) at $S(0, 0, 0, 0)$ are $\lambda_2 = -0.5437$, $\lambda_{3,4} = 0.7718 \pm 1.1151i$, respectively. Thus, system (2.2) is unstable at $S(0, 0, 0, 0)$ and in a chaotic state (see Figure 1).

The Lyapunov exponents of the system are used to further illustrate its chaos. As shown in Figure 2, the system always maintains a positive Lyapunov exponent in the early stages of evolution, which also indicates that the system is in a chaotic state, when the parameter $a = 1$, $b = 1$, $c = 1$ and the initial condition is $(1, 1, 1, 1)$.

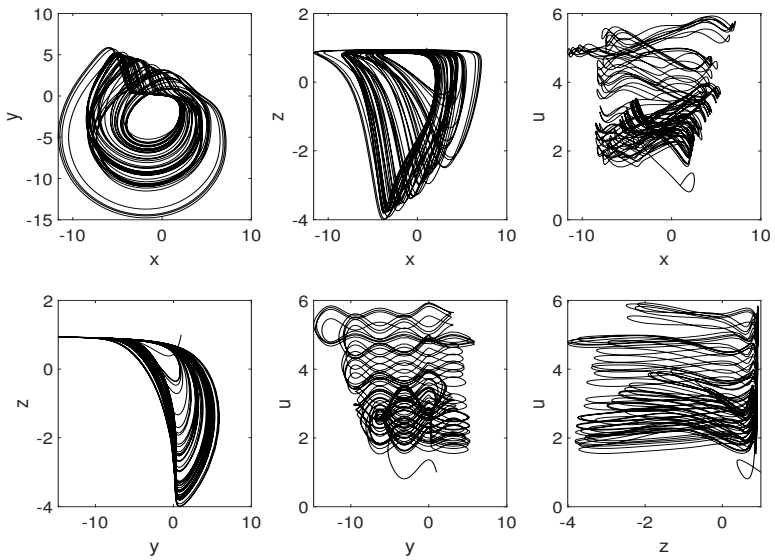

Figure 1. The chaotic attractors of the system (2.2) when $a = 1$, $b = 1$, $c = 1$, and the initial condition is (1, 1, 1, 1). (a)$O - xy$,(b)$O - xz$,(c)$O - xu$,(d)$O - yz$,(e)$O - yu$,(f)$O - zu$.

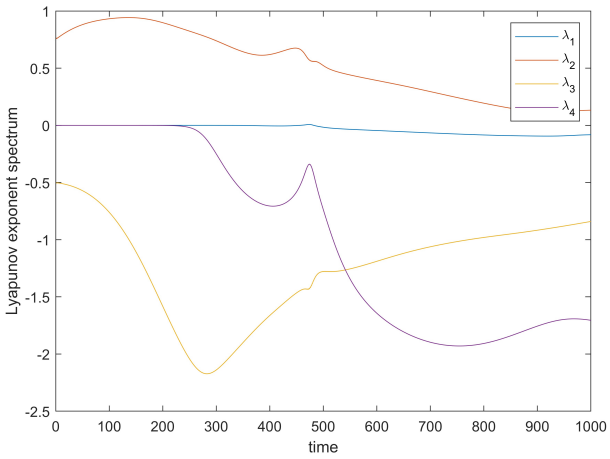

Figure 2. The Lyapunov exponents of the hyperchaos system.

3. Time-delayed feedback control of chaotic systems

In this section, we will describe the time-delay control form of system (2.2) and introduce the control principle and advantages.

To stabilize system (2.2) at the equilibrium point $S(0, 0, 0, 0)$, the time-delayed feedback control [20–22] is adopted for system (2.2) and a time-delayed feedback control method for a 4D hyperchaotic system is developed. Since time delay is an inevitable communication phenomenon in signal transmission, as well as a problem that should be considered in the balance analysis of the ecosystem, the time-delayed feedback control is conducted for the chaotic systems with coexisting attractors. Since sin(y) is the main factor causing the shared attractor, the control is expanded on the

equation of signal (u) in order to eliminate the change of the shared attractor structure and realize the control of the whole system. The form is expressed as the following time-delayed differential dynamical systems:

$$\begin{cases} \dot{x} = y + u, \\ \dot{y} = -ax + by(1 - z^2), \\ \dot{z} = -y - cz + yz, \\ \dot{u} = \sin(y) + d[y(t) - y(t - \tau)], \end{cases} \tag{3.1}$$

where d denotes the feedback gain coefficient and $\tau(\tau > 0)$ represents the delay constant. It is easy to know that the equilibrium point S of system (3.1) is consistent with that of system (2.2), thereby demonstrating that the time-delayed feedback control does not change the position and quantity of the equilibrium points of the system.

4. Main results

In this section, we will give the control process of system (2.2) and the value range of control condition parameters.

By linearizing system (2.2) at the equilibrium point $S(0, 0, 0, 0)$, the linear system is yielded:

$$\begin{cases} \dot{x} = y + u, \\ \dot{y} = -ax + by, \\ \dot{z} = -y - cz, \\ \dot{u} = d[y(t) - y(t - \tau)]. \end{cases} \tag{4.1}$$

The characteristic equation of system (4.1) is presented as:

$$\begin{vmatrix} -\lambda & 1 & 0 & 1 \\ -a & b - \lambda & 0 & 0 \\ 0 & -1 & -c - \lambda & 0 \\ 0 & d - de^{-\lambda\tau} & 0 & -\lambda \end{vmatrix} = 0. \tag{4.2}$$

Subsequently, Eq (4.2) can be transformed into:

$$\lambda^4 - b\lambda^3 + a\lambda^2 - ad\lambda - acd + (ad\lambda + acd)e^{-\lambda\tau} = 0. \tag{4.3}$$

When $\tau = 0$, system (4.1) degrades from functional differential equation to ordinary differential equation, and the stability of its equilibrium points were studied in [18]. In this study, the time-delayed feedback control of the system is considered, so the case where the time-delayed constant was positive is only considered. When $\tau > 0$, set $\lambda = i\omega(\omega > 0)$ as a pure imaginary root of the characteristic equation (4.4), and then it is substituted into the equation to separate the real and imaginary parts. The relation of ω is formed by substituting into Eq(4.4):

$$\omega^4 + b\omega^3 i - a\omega^2 - ad\omega i - acd + (ad\omega i + acd)[\cos(\omega\tau) - i\sin(\omega\tau)] = 0. \tag{4.4}$$

After separating the real and imaginary parts, the following equation set is yielded,

$$\begin{cases} acd\cos(\omega\tau) + ad\omega\sin(\omega\tau) = a\omega^2 + acd - \omega^4, \\ ad\omega\cos(\omega\tau) - acd\sin(\omega\tau) = ad\omega - b\omega^3. \end{cases} \tag{4.5}$$

In Eq (4.6), through the upper and lower equations squared, they are added together and the equation of ω is yielded to determine whether the roots of the equation exist. The Eq (4.6) can be transformed into:

$$\omega^8 + (b^2 - 2a)\omega^6 + (a^2 - 2acd - 2abd)\omega^4 + 2a^2cd\omega^2 = 0. \tag{4.6}$$

Additionally, since $\omega > 0$, Eq (4.7) continued to be transformed and the root is extracted.

$$\omega^6 + (b^2 - 2a)\omega^4 + (a^2 - 2acd - 2abd)\omega^2 + 2a^2cd = 0. \tag{4.7}$$

Theorem 1. *If $d < 0$, Eq (4.7) has at least one positive real root.*

Proof. Let $\upsilon = \omega^2$, The auxiliary function $\varphi(\upsilon)$ is constructed through Eq (4.7), then it can be expressed as:

$$\varphi(\upsilon) = \upsilon^3 + (b^2 - 2a)\upsilon^2 + (a^2 - 2acd - 2abd)\upsilon + 2a^2cd.$$

Next, $\varphi(\upsilon)$ can be transformed into:

$$\varphi(\upsilon) = \frac{1 + (b^2 - 2a)\frac{1}{\upsilon} + (a^2 - 2acd - 2abd)\frac{1}{\upsilon^2} + 2a^2cd\frac{1}{\upsilon^3}}{\frac{1}{\upsilon^3}}.$$

If $\varphi(\upsilon)$ meets the zero-existence theorem, it can be known that $\varphi(\upsilon)$ has real roots because

$$\varphi(0) = 2a^2cd < 0, \lim_{\upsilon\to\infty} \varphi(\upsilon) = +\infty.$$

Subsequently, $\varphi(\upsilon)$ has real roots on $(0, +\infty)$. Accordingly, the equation has at least one positive real root, and the proof ends.

It is assumed that the roots of Eq (4.7) are denoted as ω_0. According to Eq (4.6), the following Eq (4.5) can be obtained:

$$\begin{cases} \sin(\omega_0\tau) = \frac{ad\omega_0(a\omega_0^2+acd-\omega_0^4)-acd(ad\omega_0-b\omega_0^3)}{(ad\omega_0)^2+(acd)^2}, \\ \cos(\omega_0\tau) = \frac{acd(a\omega_0^2+acd-\omega_0^4)+ad\omega_0(ad\omega_0-b\omega_0^3)}{(ad\omega_0)^2+(acd)^2}. \end{cases} \tag{4.8}$$

After substituting $\omega = \omega_0$ into Eq (4.8), the value of the time delay τ is yielded as:

$$\tau_k = \begin{cases} \frac{1}{\omega_0}[\arccos(Q_k) + 2j\pi], P_k \geq 0, \\ \frac{1}{\omega_0}[2\pi - \arccos(Q_k) + 2j\pi], P_k < 0, \end{cases} \quad j = 0, 1, 2, \cdots \tag{4.9}$$

where

$$\begin{cases} P_k = \sin(\omega_0\tau) = \frac{ad\omega_0(a\omega_0^2+acd-\omega_0^4)-acd(ad\omega_0-b\omega_0^3)}{(ad\omega_0)^2+(acd)^2}, \\ Q_k = \cos(\omega_0\tau) = \frac{acd(a\omega_k^2+acd-\omega_0^4)+ad\omega_0(ad\omega_0-b\omega_0^3)}{(ad\omega_0)^2+(acd)^2}. \end{cases}$$

When the roots of Eq (4.8) are (ω_0, τ_0), i.e., the time delay $\tau = \tau_0$, Eq (4.4) has conjugate pure virtual roots $\lambda = \pm i\omega_0$. It is assumed that when $\tau_0 = \min\{\tau_0\}$, the pure imaginary roots of Eq (4.4) are $\lambda = \pm i\omega_0$ then the following conclusions can be drawn. □

Theorem 2. *If $a > 0$, $b > 0$, $0 < c < \pi$, $d < 0$ and $\tau = \tau_0$, the equation has a pair of pure imaginary roots $\lambda = \pm i\omega_0$.*

The eigenvalues of Eq (4.4) are assumed as $\lambda(\tau) = \alpha(\tau) + i\omega(\tau)$, which satisfy $\alpha(\tau_k) = 0$ and $\omega(\tau_0) = \omega_0$, and the transversality conditions are presented below. On the basis of Eq (4.6), set $x = \omega^2$, and then an auxiliary function $f(x)$ is built as:

$$f(x) = x^4 + (b^2 - 2a)x^3 + (a^2 - 2acd - 2abd)x^2 + 2a^2cdx.$$

Theorem 3. *If $a > 0$, $b > 0$, $0 < c < \pi$, $d < 0$, and $f'(\omega_0^2) \neq 0$, then $\frac{d\mathrm{Re}\lambda(\tau)}{d\tau}\Big|_{\tau=\tau_k} \neq 0$.*

Proof. After taking the derivatives of both sides of the characteristic equation (4.4) related to τ, the following equation can be obtained:

$$[4\lambda^3 - 3b\lambda^2 + 2a\lambda - ad + ade^{-\lambda\tau} - \tau(ad\lambda + acd)e^{-\lambda\tau}]\frac{d\lambda}{d\tau} = \lambda(ad\lambda + acd)e^{-\lambda\tau}. \tag{4.10}$$

Based on the mentioned Eq (4.4), the following equation can be obtained:

$$(ad\lambda + acd)e^{-\lambda\tau} = -(\lambda^4 - b\lambda^3 + a\lambda^2 - ad\lambda - acd). \tag{4.11}$$

After substituting (4.11) into (4.10), the following equation can be yielded:

$$\begin{aligned}(\frac{d\lambda}{d\tau})^{-1} &= \frac{4\lambda^3 - 3b\lambda^2 + 2a\lambda - ad}{\lambda(ad\lambda + acd)e^{-\lambda\tau}} + \frac{ade^{-\lambda\tau}}{\lambda(ad\lambda + acd)e^{-\lambda\tau}} - \frac{\tau(ad\lambda + acd)e^{-\lambda\tau}}{\lambda(ad\lambda + acd)e^{-\lambda\tau}} \\ &= -\frac{4\lambda^3 - 3b\lambda^2 + 2a\lambda - ad}{\lambda(\lambda^4 - b\lambda^3 + a\lambda^2 - ad\lambda - acd)} + \frac{ad}{\lambda(ad\lambda + acd)} - \frac{\tau}{\lambda}.\end{aligned} \tag{4.12}$$

When $\tau_k = \tau_0$, $\lambda = i\omega_0$, and then λ is substituted into (4.12):

$$\begin{aligned}\mathrm{Re}[(\frac{d\lambda}{d\tau})^{-1}\Big|_{\tau=\tau_k}] &= -\mathrm{Re}[\frac{4\lambda^3 - 3b\lambda^2 + 2a\lambda - ad}{\lambda(\lambda^4 - b\lambda^3 + a\lambda^2 - ad\lambda - acd)}\Big|_{\tau=\tau_k}] + \mathrm{Re}[\frac{ad}{\lambda(ad\lambda + acd)}\Big|_{\tau=\tau_k}] \\ &= -\mathrm{Re}[\frac{3b\omega_0^2 - ad + (2a\omega_0 - 4\omega_0^3)i}{ad\omega_0^2 - b\omega_0^4 + (\omega_0^5 - a\omega_0^3 - acd\omega_0)i)}] + \mathrm{Re}(\frac{ad}{-ad\omega_0^2 + acd\omega_0 i)}) \\ &= \frac{(3b\omega_0^2 - ad)(b\omega_0^2 - ad) + (4\omega_0^2 - 2a)(\omega_0^4 - a\omega_0^2 - acd)}{(ad\omega_0 - b\omega_0^3)^2 + (\omega_0^4 - a\omega_0^2 - acd)^2} + \frac{-a^2d^2}{a^2d^2\omega_0^2 + a^2d^2c^2}.\end{aligned} \tag{4.13}$$

Moreover, after substituting λ into Eq (4.4), the following equation can be developed:

$$\omega_0^4 + b\omega_0^3 i - a\omega_0^2 - ad\omega_0 i - acd + (ad\omega_0 i + acd)e^{-i\omega_0\tau_0} = 0. \tag{4.14}$$

As $e^{-i\omega_0\tau_0} = \cos\omega_0\tau_0 - i\sin\omega_0\tau_0$, so $\left|e^{-i\omega_0\tau_0}\right| = 1$. Thus, the following equation can be obtained:

$$\left|\omega_0^4 + b\omega_0^3 i - a\omega_0^2 - ad\omega_0 i - acd\right| = \left|ad\omega_0 i + acd\right|.$$

That is,

$$(ad\omega_0 - b\omega_0^3)^2 + (\omega_0^4 - a\omega_0^2 - acd)^2 = a^2d^2\omega_0^2 + a^2d^2c^2. \tag{4.15}$$

After combining (4.13) and (4.15), the following equation can be obtained:

$$\mathrm{Re}[(\frac{d\lambda}{d\tau_1})^{-1}\Big|_{\tau=\tau_k}] = \frac{f'(\omega_0^2)}{(ad\omega_0 - b\omega_0^3)^2 + (\omega_0^4 - a\omega_0^2 - acd)^2} \neq 0.$$

As

$$Sign[\mathrm{Re}(\frac{d\lambda}{d\tau}\Big|_{\tau=\tau_k})] = Sign\{\mathrm{Re}[(\frac{d\lambda}{d\tau})^{-1}\Big|_{\tau=\tau_k}]\},$$

the theorem is proved. □

Accordingly, by Theorem 3 and the Hopf bifurcation theory, the following conclusions are drawn.

Theorem 4. *If $a > 0$, $b > 0$, $0 < c < \pi$, $d < 0$ and $f'(\omega_0^2) \neq 0$, then*

(1) When $\tau \in [0, \tau_0)$, the equilibrium point $O(0, 0, 0)$ of the system (4.1) is asymptotically stable;

(2) When $\tau > \tau_0$, the equilibrium point $O(0, 0, 0)$ of the system (4.1) turns out to be unstable;

(3) $\tau = \tau_k (k = 0, 1, 2)$ is the Hopf bifurcation value of the system (4.1), i.e., the system (4.1) has Hopf bifurcation at the equilibrium point $O(0, 0, 0)$.

5. Numerical example

In this section, we will give an example to demonstrate the proposed time-feedback control effectiveness.

To study the stability of the system at the equilibrium point and examine the three conditions of Theorem 4, the parameters in system (4.1) are valued and simulated in the following. According to the conditions in Theorem 4, the system parameters of system (4.1) were set as $a = 1$, $b = 1$, $c = 1$, $d = -1$, respectively. In this case, the system was written as:

$$\begin{cases} \dot{x} = y + u, \\ \dot{y} = -x + y(1 - z^2), \\ \dot{z} = -y - z + yz, \\ \dot{u} = \sin(y) - [y(t) - y(t - \tau)]. \end{cases} \tag{5.1}$$

The positive real roots of Eq (4.7) were obtained using mathematical software. On that basis, a pair of conjugate eigenroots $\pm 0.4749i$ existed in the characteristic equation. Subsequently, $f'(\omega_0^2) = -0.0278 \neq 0$. Moreover, in Eq (4.10), $\tau_0 = 0.6485$. Based on the above calculations and the systematic expressions, the inferences of Theorem 4 were obtained.

Corollary 1. *If $a > 0$, $b > 0$, $0 < c < \pi$, $d < 0$ and $f'(\omega_0^2) \neq 0$, then*

(1) When $\tau \in [0, 0.6485)$, the equilibrium point of system (5.1) was asymptotically stable.

(2) When $\tau = 0.6485 + 3.0840k\pi (k = 0, 1, 2, 3, \cdots)$, the Hopf bifurcation occurred near the equilibrium point $O(0, 0, 0, 0)$ of system (5.1), and periodic solutions appeared.

This study still takes the initial condition of the system $(x_0, y_0, z_0, u_0) = (1, 1, 1, 1)$ as an example, and the stability of the system was simulated under different time-delayed constants. Next, the mathematical software was used to draw the trajectory diagram and phase diagram of the system's state variables over time when the time delay τ took different values (see Figures 3 and 4), thereby verifying the correctness of the obtained results.

Figure 3 indicates that when $\tau = 0.6485$, the state variables of the system x, y, z always kept periodic oscillations over time t. According to Figure 4, limit cycles appeared in both $O - xyz$ space and $O - xyz$ space, which demonstrates that the system had the Hopf bifurcation at the equilibrium point $O(0, 0, 0)$.

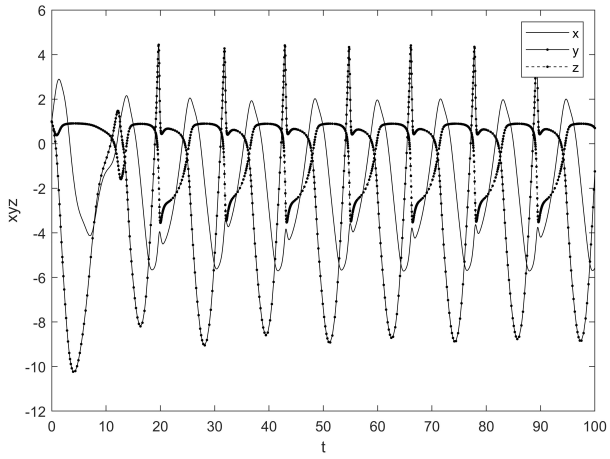

Figure 3. The change curve of the system's state variables over time with the time delay of 0.6485 and with the initial condition of (1,1,1,1).

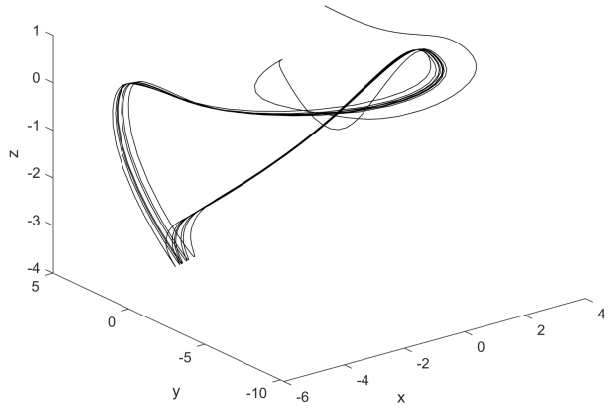

Figure 4. $O - xyz$ phase diagram of the system with the time delay of 0.6485 and initial conditions of (1,1,1,1).

The time-delayed value was changed to get the results (see Figure 5). As shown in Figure 5, when $\tau = 0.2$, the system was asymptotically stable at the equilibrium point $O(0, 0, 0)$. The initial conditions $(x_0, y_0, z_0, u_0) = (2.5, 0, 0, 0)$ were altered, and then the simulation experiment was continued. The results are illustrated in Figures 6–8.

According to Figures 6–8, the dynamic behaviors of the system are still consistent with our expectations. Under arbitrary initial conditions, the dynamic behaviors of the system were effectively controlled under the time-delayed feedback control, which demonstrates that the proposed method also exhibits effectiveness on complex high-dimensional hyperchaotic systems.

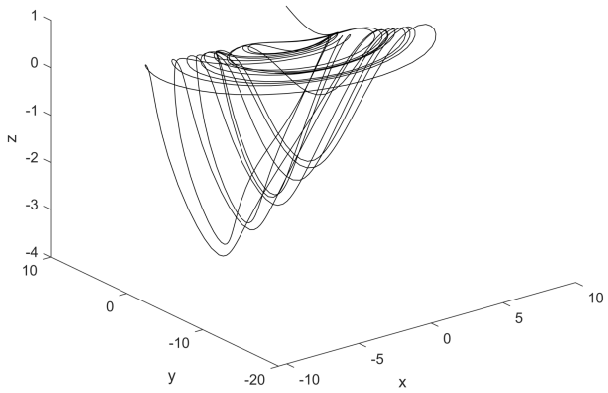

Figure 5. $O-xyz$ phase diagram of the system with the time delay of 0.2 and initial conditions of (1,1,1,1).

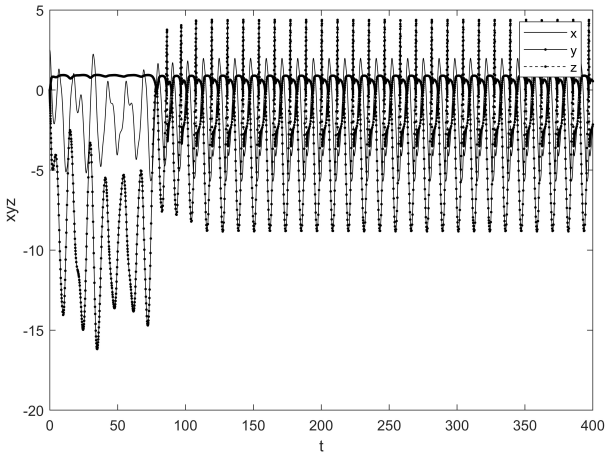

Figure 6. The change curve of the system's state variables with the time delay of 0.6485 and with the initial condition of (2.5,0,0,0).

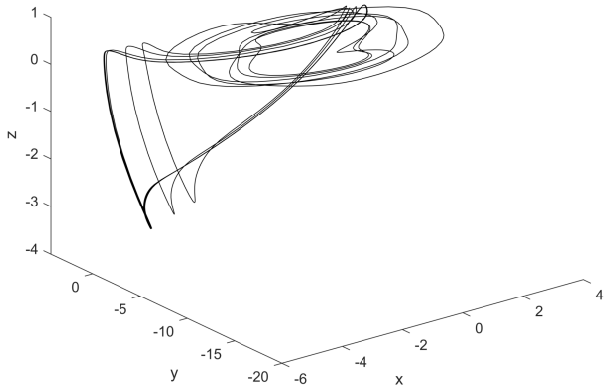

Figure 7. $O-xyz$ phase diagram of the system with the time delay of 0.6485 and initial conditions of (2.5,0,0,0).

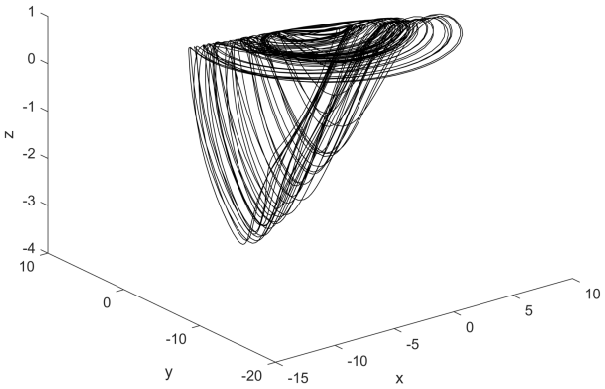

Figure 8. $O-xyz$ phase diagram of the system with the time delay of 0.2 and initial conditions of (2.5,0,0,0).

By using the method of the Poincar é section to draw the bifurcation diagram of the controlled system with respect to τ, the correctness of the conclusion is further verified. Take the trajectory of the controlled system within the time distribution interval of [30,60] and use section x-y=0 to intercept the point set in the O-xyz space of the controlled system to draw the bifurcation diagram of the system, as shown in Figure 9. According to Figure 9, the controlled system entered a chaotic state near $\tau = 0.6485$.

As shown in Figure 10, a graph of the variation of state variable y with time t was drawn and chaos control was performed on the system at $t = 100$. It can be clearly observed that the system is well controlled at $\tau = 0.1$.

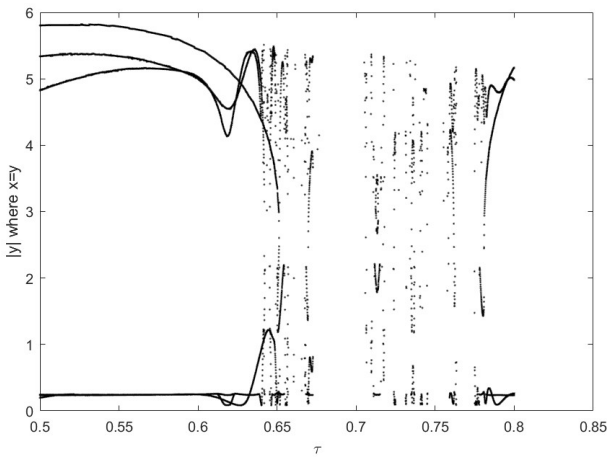

Figure 9. The bifurcation diagram of the controlled system with respect to τ.

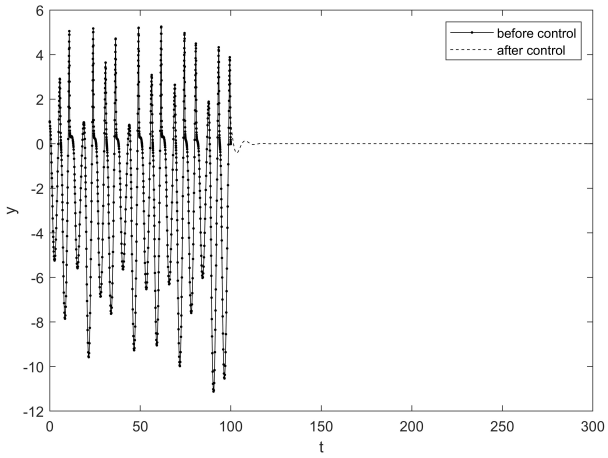

Figure 10. Control effectiveness of controlled systems.

6. Conclusions

In this study, the time-delayed feedback control was conducted to the high-dimensional hyperchaos system. The controlled hyperchaos system refers to a functional differential dynamic system with any number of coexisting attractors. Subsequently, through the root distribution of the characteristic equation of a linear system, the effect of the time-delayed value on the equilibrium point of the system was analyzed, as well as the parameters and time delay conditions of the system having the Hopf bifurcation close to the equilibrium point. The research results of this study can be considered to further extend the research on the controlled 3D chaotic systems, which are of high theoretical and application significance.

Use of AI tools declaration

The author declares he has not used Artificial Intelligence (AI) tools in the creation of this article.

Acknowledgments

Some of the authors of this publication are also working on these related projects: (1) Jiangsu Science and Technology Think Tank Youth Talent Program under grant no.2023(JSKJZK2023068). (2) Jiangsu Province Higher Vocational Education high-level Professional Group Construction Project Funding (Su Teaching Letter (2021) No. 1). (3) Jiangsu Province Vocational Education Teacher Teaching Innovation Team (Su Teaching Office Letter (2021) No. 23). (4) Engineering Technology Research and Development Center of Jiangsu Higher Vocational Colleges (Su Jiaoke Letter (2023) No. 11). (5) Excellent Scientific and Technological Innovation Team of Jiangsu Universities (Su Jiaoke (2023) No. 3).

Conflict of interest

The author declares no conflict of interest.

References

1. K. Cheng, Z. Lu, Y. Zhen, Multi-level multi-fidelity sparse polynomial chaos expansion based on Gaussian process regression, *Comput. Meth. Appl. Mech. Eng.*, **349** (2019), 360–377. https://doi.org/10.1016/j.cma.2019.02.021
2. G. C. Wu, D. Baleanu, Discrete chaos in fractional delayed logistic maps, *Nonlinear Dyn.*, **80** (2014), 1697–1703. https://doi.org/10.1007/s11071-014-1250-3
3. L. Grigoryeva, A. Hart, J. P. Ortega, Chaos on compact manifolds: differentiable synchronizations beyond Takens, *Phys. Rev. E*, **103** (2020), 062204. https://doi.org/10.1103/PhysRevE.103.062204
4. A. Jahangiri, N. K. A. Attari, A. Nikkhoo, Z. Waezi, Nonlinear dynamic response of an Euler-Bernoulli beam under a moving mass-spring with large oscillations, *Arch. Appl. Mech.*, **90** (2020), 1135–1156. https://doi.org/10.1007/s00419-020-01656-9
5. F. Fotiadis, K. G. Vamvoudakis, Detection of actuator faults for continuous-time systems with intermittent state feedback, *Syst. Control Lett.*, **152** (2021), 104938. https://doi.org/10.1016/j.sysconle.2021.104938
6. T. Xu, J. Xu, X. Zhang, Inertia-free computation efficient immersion and invariance adaptive tracking control for Euler-Lagrange mechanical systems with parametric uncertainties, *Adv. Space Res.*, **66** (2020), 1902–1910. https://doi.org/10.1016/j.asr.2020.07.004
7. M. P. Aghababa, No-chatter variable structure control for fractional nonlinear complex systems, *Nonlinear Dyn.*, **73** (2013), 2329–2342. https://doi.org/10.1007/s11071-013-0944-2
8. X. Song, L. Chen, K. Wang, D. He, Robust time-delay feedback control of vehicular CACC systems with uncertain dynamics, *Sensors*, **20** (2020), 1775. https://doi.org/10.3390/s20061775
9. M. Farazmand, Mitigation of tipping point transitions by time-delay feedback control, *Chaos*, **301** (2019), 013149. https://doi.org/10.1063/1.5137825
10. Y. Ding, L. Zheng, R. Yang, Time-delayed feedback control of improved friction-induced model: application to moving belt of particle supply device, *Nonlinear Dyn.*, **100** (2020), 423–434. https://doi.org/10.1007/s11071-020-05523-8
11. G. Yang, Hopf birurcation of Lorenz-like system about parameter *h*, *Mod. Appl. Sci.*, **4** (2009), 91–95. https://doi.org/10.5539/mas.v4n1p91
12. Y. Li, H. P. Ju, C. Hua, G. Liu, Distributed adaptive output feedback containment control for time-delay nonlinear multiagent systems, *Automatica*, **127** (2021), 109545. https://doi.org/10.1016/j.automatica.2021.109545
13. J. Kengne, Z. T. Njitacke, H. B. Fotsin, Dynamical analysis of a simple autonomous jerk system with multiple attractors, *Nonlinear Dyn.*, **83** (2016), 751–765. https://doi.org/10.1007/s11071-015-2364-y
14. V. T. Pham, C. Volos, S. Jafari, T. Kapitaniak, Coexistence of hidden chaotic attractors in a novel no-equilibrium system, *Nonlinear Dyn.*, **87** (2017), 2001–2010. https://doi.org/10.1007/s11071-016-3170-x

15. B. C. Bao, H. Bao, N. Wang, M. Chen, Q. Wu, Hidden extreme multistability in memristive hyperchaotic system, *Chaos Soliton. Fract.*, **94** (2017), 102–111. https://doi.org/10.1016/j.chaos.2016.11.016
16. B. Bao, W. Ning, X. Quan, H. Wu, Y. Hu, A simple third-order memristive band pass filter chaotic circuit, *IEEE Trans. Circuits Syst. II*, **64** (2017), 977–981. https://doi.org/10.1109/TCSII.2016.2641008
17. C. Li, W. J. C. Thio, J. C. Sprott, H. H. C. Iu, Y. Xu, Constructing infinitely many attractors in a programmable chaotic circuit, *IEEE Access*, **2018** (2018), 29003–29012. https://doi.org/10.1109/ACCESS.2018.2824984
18. Q. Lai, Z. Wan, P. D. K. Kuate, H. Fotsin, Coexisting attractors, circuit implementation and synchronization control of a new chaotic system evolved from the simplest memristor chaotic circuit, *Commun. Nonlinear Sci. Numer. Simul.*, **89** (2020), 105341. https://doi.org/10.1016/j.cnsns.2020.105341
19. B. Muthuswamy, L. O. Chua, Simplest chaotic circuit, *Int. J. Bifurcation Chaos*, **20** (2010), 1567–1580. https://doi.org/10.1142/S0218127410027076
20. X. Zhang, Y. Lin, Global stabilization of high-order nonlinear time-delay systems by state feedback, *Syst. Control Lett.*, **65** (2014), 89–95. https://doi.org/10.1016/j.sysconle.2013.12.015
21. C. C. Hua, X. P. Guan, Smooth dynamic output feedback control for multiple time-delay systems with nonlinear uncertainties, *Automatica*, **28** (2016), 1–8. https://doi.org/10.1016/j.automatica.2016.01.007
22. E. Fridman, U. Shaked, A descriptor system approach to H∞ control oflinear time-delay systems, *IEEE Trans. Autom. Control*, **47** (2002), 253–270. https://doi.org/10.1109/9.983353

AIMS Press